Axial-Ligand-Cleavable Silicon Phthalocyanines Triggered by Near-Infrared Light toward Design of Photosensitizers for Photoimmunotherapy

Hideo Takakura
Hokkaido Univeristy
Shino Matsuhiro
Hokkaido Univeristy
Masato Kobayashi
Hokkaido University
Yuto Goto
Hokkaido University
Mei Harada
Hokkaido University
Tetsuya Taketsugu
Hokkaido University
Mikako Ogawa (mogawa@pharm.hokudai.ac.jp)
Hokkaido University

Article

Keywords: Near-infrared photoimmunotherapy (NIR-PIT), IRDye700DX (IR700), silicon phthalocyanine (SiPc), near-infrared (NIR), HER2

Posted Date: September 20th, 2021

DOI: https://doi.org/10.21203/rs.3.rs-904362/v1

Axial-Ligand-Cleavable Silicon Phthalocyanines Triggered by Near-Infrared Light toward Design of Photosensitizers for Photoimmunotherapy

Hideo Takakura[1], Shino Matsuhiro[1], Masato Kobayashi[2,3], Yuto Goto[1], Mei Harada[1], Tetsuya Taketsugu[2,3], Mikako Ogawa*[1]

[1] Laboratory of Bioanalysis and Molecular Imaging, Graduate School of Pharmaceutical Sciences, Hokkaido University, Sapporo, Hokkaido, Japan

[2] Faculty of Science, Hokkaido University, Sapporo, Hokkaido, Japan

[3]WPI-ICReDD, Hokkaido University, Sapporo, Hokkaido, Japan

*Corresponding author: Mikako Ogawa

Laboratory of Bioanalysis and Molecular Imaging, Graduate School of Pharmaceutical Sciences, Hokkaido University, Sapporo, Hokkaido 060-0812, Japan

Phone: +81-11-706-3767, Fax: +81-11-706-3767.

E-mail: mogawa@pharm.hokudai.ac.jp

Abstract

Near-infrared photoimmunotherapy (NIR-PIT) is a novel phototherapy for the treatment of cancer that uses NIR light and conjugates of antibody-IR700, a silicon phthalocyanine photosensitizer. A key feature of NIR-PIT is light-induced axial ligand cleavage of IR700, which finally causes cytotoxicity. Here, we focused on protonation of the axial ligand on the IR700 anion radical during the photochemical process. The Gibbs energy in the protonation reaction of IR700 derivatives with different axial ligands was calculated. These calculations suggested the order of the cleavage efficiency corresponds to the basicity of the axial ligand (*i.e.* alkoxy > siloxy (IR700) > phenoxy ≈ oxycarbonyl), which was confirmed by the photoirradiation experiments with synthesized compounds. Thus, axial ligand cleavage is significantly dependent on the basicity of the axial ligand. Our findings suggest that PIT reagent with an IR700 derivative bearing alkoxy group would show better efficacy than IR700.

Introduction

IRDye700DX (IR700) is a silicon phthalocyanine (SiPc) derivative that absorbs near-infrared (NIR) light and has been used not only as a fluorescent imaging reagent but also as a photosensitizer for NIR photoimmunotherapy (NIR-PIT) (Fig. 1a).[1,2] In NIR-

PIT, IR700-antibody conjugate and NIR light are used to treat cancer. Because the cytotoxicity is induced only when the conjugate is bound to the cell membrane and irradiated with NIR light, NIR-PIT can specifically kill cancer cells. To date, various cancer antigens, such as epidermal growth factor receptor (EGFR) and human epidermal growth factor receptor 2 (HER2), have been targeted. In pre-clinical experiments, NIR-PIT has shown efficacy against gastric,[3,4] lung,[5] prostate,[6] and breast[7] cancers. In addition, successful first-in-human phase I and II studies in patients with unresectable locally advanced head and neck cancer were completed (NCT02422979). More recently, Cetuximab-IR700, a PIT conjugate for EGFR, was approved in Japan. These studies suggest PIT will be a valuable new form of cancer treatment.

Because light is attenuated by tissue absorption and scattering, PIT utilizes NIR light delivered through a thin fiber, such as a catheter or needle, to increase the efficiency of light delivery at deep sites. Moreover, cytotoxicity should be further enhanced by using a light-sensitive photosensitizer that is more responsive to NIR light. However, only IR700 has been reported as a photosensitizer for PIT. Therefore, it remains unclear whether IR700 is the optimal photosensitizer for this treatment. Recently, the mechanism of cytotoxicity in PIT has been investigated both experimentally and theoretically. As shown in Fig. 1b, IR700 is excited to the singlet excited state by NIR light, and then

55 transitions to the triplet state via intersystem crossing (ISC). However, the quantum yield
56 of ISC is not high (Φ_{ISC} = 0.019).[8] IR700 in the triplet state receives electrons from
57 electron donors to form the anion radical. Next, the anion radical is protonated by a
58 hydronium ion, followed by axial ligand cleavage and the coordination of a hydroxy ion,
59 which occur spontaneously at room temperature due to the lower activation energy of the
60 photochemical process ($E^{\ddagger}$ < 92.4 kJ mol^{-1}).[9,10] The photodegraded compound loses its
61 hydrophilic functional moiety (*i.e.* six sulfonate groups in all), which drastically changes
62 its physicochemical properties from water-soluble to insoluble. As a result, the conjugate
63 aggregates on the cell membrane, leading to physical damage and ultimately cell
64 death.[11,12] Thus, axial ligand cleavage of the photosensitizer is a crucial step in PIT. The
65 development of a light-sensitive photosensitizer involves the design of SiPcs in which the
66 axial ligand is more readily cleaved by NIR light.
67 Previously, we conducted experiments that showed the efficiency of axial ligand
68 cleavage by NIR light is dependent on the pH of the solution.[9] At higher pH, light-induced
69 cleavage of the axial ligand was inhibited because protonation of the SiPc anion radical
70 did not occur. These results suggested that axial ligand cleavage is dependent on the
71 basicity of axial ligand. Thus, in order to develop an SiPc derivative that is more light-
72 sensitive than IR700, we focused on the basicity of the axial ligands. Here, the basicity

of SiPcs with various axial ligands was estimated by performing quantum chemical calculations. The compounds were then synthesized, and light-induced axial ligand cleavage was compared.

Results and discussions

Quantum chemical calculations of SiPcs with different axial ligands in photoinduced axial ligand cleavage. We reported that in the presence of an electron donor under hypoxic conditions, the axial ligand of the IR700 derivative cleaves at pH 7.0, while at pH 11.0 no cleavage of the axial ligand occurs despite the generation of an anion radical.[9] This result motivated us to investigate the reactivity of SiPcs having other axial ligands with a different basicity. Rather than a siloxy group as the axial ligand, we chose alkoxy, oxycarbonyl and phenoxy groups because they show a different basicity and are functional groups capable of forming an Si-O bond (Fig. 2a). As in our previous study, symmetric SiPc derivatives were used as model compounds for the calculations (compounds **1**'-**4**', Fig. 2b).[9] Density functional theory (DFT) calculations were performed to determine the change in Gibbs energy (ΔG) of each compound (**1**'-**4**') for the following protonation reaction of the axial ligand at 298.15 K:

$$[SiPcY_2]^{\bullet-} + H_3O^+ \rightarrow [SiPc(YH)Y]^{\bullet} + H_2O \qquad (1)$$

where Y = $OSiMe_3$ (**1**'), OEt (**2**'), OCOEt (**3**'), and OPh (**4**'). The calculated ΔG is also summarized in Fig. 2b. As for the oxycarbonyl axial ligand, protonation of the carbonyl oxygen was considered because it is more basic than the ester oxygen. All ΔG values are negative, indicating that the reaction (1) is exergonic. The order of ΔG for each compound was compound **2**' (alkoxy) < compound **1**' (siloxy) < compound **4**' (phenoxy) ≈ compound **3**' (oxycarbonyl). If we assume equilibration between the anion radical form ($[SiPcY_2]^{\bullet-}$) and the protonated form ($[SiPc(YH)Y]^{\bullet}$) in solution, these results suggest the protonated form of the alkoxy ligand is favored over the other ligands and has more opportunity to proceed with the ligand cleavage reaction. However, the result differs from a previous report that investigated SiPcs having an asymmetric axial ligand, alkoxy and phenoxy groups.[13] The previous study concluded that the axial ligand of a phenoxy group cleaves more readily upon NIR light irradiation than an alkoxy group. This apparent discrepancy might arise because (i) the concerted hydrolysis reaction pathway has an activation energy of approximately 30 kJ mol^{-1} higher than the stepwise pathways considered in this study, and (ii) symmetrical differences in the axial ligand (*i.e.* symmetric versus asymmetric). Our results suggest the anticipated efficiency of axial ligand cleavage to be: compound **2** > compound **1** > compound **4** ≈ compound **3**. The detailed energy diagram for the formation of $[SiPc(OH)Y]^{\bullet-}$ from $[SiPcY_2]^{\bullet-}$ in neutral

water solution (summarized in our previous report for the case of Y = $OSiMe_3$) is shown in supporting information (see Supplementary Fig. 1).

Synthesis and photochemical properties of the SiPcs with different axial ligands. Given the above results, we synthesized compounds **2**-**4** (Fig. 2a) to experimentally evaluate the predictions based on the theoretical calculations. As shown in Figure 3, the axial ligands were conjugated via SiPc dichloride (**6**) using sodium hydride or K_2CO_3 as a base. Final products containing a water-soluble group at the end of the axial ligand were synthesized in MeOH with sultone. Compounds **2**-**4** were characterized by ^{1}H NMR and MS. To investigate whether the axial ligands of SiPc affect their photochemical properties, we measured the absorption/emission spectra and determined the fluorescence quantum yields (Φ_{FL}) and the molar extinction coefficients (ε). All the compounds showed almost identical photochemical properties (see Supplementary Fig. 2 and Table 1). Compounds **1**-**4** displayed similar shaped absorption and emission spectra with a sharp Q-band absorption peak in the range of 677-691 nm and a sharp emission peak in the range of 684-699 nm. The relative Φ_{FL} of compounds **2**-**4** were calculated with reference to the absolute Φ_{FL} of compound **1** (Φ_{FL} = 0.31).[8] As a result, Φ_{FL} of compounds **2**-**4** were 0.30, 0.27 and 0.29, respectively. Furthermore, ε at the Q-band of compounds **1**-**4** in water were

1.7-1.9 × 10^5 L mol^{-1} cm^{-1}. These results indicate the axial ligands do not significantly affect the photochemical properties of the SiPc derivatives.

Comparison of photoinduced axial ligand cleavage reaction of synthesized SiPcs. With these compounds in hand, we investigated the axial ligand photocleavage of compounds **1**-**4**. The compounds in a phosphate buffer with dithiothreitol (DTT) as an electron donor were irradiated with an NIR laser (690 nm) at different light doses. After irradiation, the solutions were analyzed by HPLC with methylene blue as an internal standard. NIR light irradiation of compounds **1**-**4** caused the peaks of the original compound to decrease and other peaks to appear (Fig. 4a-d). Indeed, as the light dose increased, the peaks of the original compounds disappeared. The degradation products of compound **1**, named degrade 1a and 1b, were previously identified as SiPc with one or both ($SiPc(OH)_2$) of the axial ligands cleaved, respectively (Fig. 4e).[10] The other degradation products, degrade 2b, 3a and 4a, were also analyzed by double injection with authentic compound $SiPc(OH)_2$. In each case the degradation product was identified as $SiPc(OH)_2$, as with compound **1** (see Supplementary Fig. 3). Based on these findings, degrade 2a was expected to be SiPc with uniaxial ligand. Thus, we synthetically prepared the compound (compound **2**-half) from compound **2** (Fig. 4e and see Supplementary

145 Scheme 1). Using the authentic compound, degrade 2a was identified as compound **2**-half
146 (see Supplementary Fig. 3). In the case of no NIR irradiation, compounds **1**-**4** did not
147 degrade at all (see supplementary Fig. 4). These results show that the axial ligands of
148 compounds **2**-**4** are cleaved by NIR irradiation in the presence of an electron donor, as in
149 compound **1**.

150 The cleavage of the axial ligands was categorized into two types. For compounds
151 **1** and **2**, peaks corresponding to SiPc with uniaxial ligand (degrades 1a, 2a) was observed,
152 which disappeared upon increasing light dose together with a concomitant increase in the
153 appearance of $SiPc(OH)_2$ (degrades 1b, 2b) (Fig. 4a,b). By contrast, for compounds **3** and
154 **4**, light irradiation resulted in the formation of $SiPc(OH)_2$ (degrades 3a, 4a), but no peaks
155 corresponding to SiPc with uniaxial ligand (Fig. 4c,d). When compounds **3** and **4** were
156 hydrolyzed in aqueous solution at pH11-12, peaks of compounds **3** and **4** with uniaxial
157 ligand were not detected but that of $SiPc(OH)_2$ was detected (see Supplementary Fig. 5).
158 On the other hand, in the hydrolysis of compounds **1** and **2**, peaks of compounds **1** and **2**
159 with uniaxial ligand were detected. These results suggest compounds **3** and **4** with
160 uniaxial ligand might be unstable in aqueous solution. Another possibility is that in the
161 case of compounds **3** and **4**, the two axial ligands were sequentially cleaved in the
162 photochemical reaction, whereas cleavage of the axial ligand of compounds **1** and **2**

occurred one by one. Thus, the change in ΔG for the protonation reaction to the second axial ligand, namely,

$$[SiPc(OH)Y]^{\bullet-} + H_3O^+ \rightarrow [SiPc(YH)(OH)]^{\bullet} + H_2O \quad (2)$$

was obtained from the DFT calculations (see Supplementary Fig. 6). Comparison with Fig. 2(b) shows the ΔG of eq (2) for oxycarbonyl and phenoxy ligands are 7.8 and 0.3 kJ mol^{-1} lower than those of eq (1), respectively. By contrast, the ΔG of eq (2) for siloxy and alkoxy ligands are 4.5 and 4.6 kJ mol^{-1} higher than eq (1), respectively. This observation supports the sequential cleavage of compounds **3** and **4**.

Next, we compared the efficiency of axial ligand cleavage for the synthesized compounds **1**-**4**. Because $SiPc(OH)_2$ is hydrophobic with limited solubility in aqueous solution, most of the reaction product precipitated. Thus, although the dissolved portion of $SiPc(OH)_2$ was detected by HPLC, we could not quantify axial ligand cleavage from the peak areas of $SiPc(OH)_2$. Therefore, comparison of the reaction efficiency was performed from the decrease in the peak areas of compounds **1**-**4**. As anticipated from the theoretical calculations, the order of efficiency was compound **2** > compound **1** > compound **4** ≈ compound **3**, consistent with the order of ΔG of the anion radicals upon protonation (Fig. 4f). These results show that the ΔG value correlated with the efficiency of axial ligand cleavage. Specifically, the basicity of the axial ligand was related to the

dissociation efficiency. Thus, we successfully developed compound **2** with an axial ligand comprising an alkoxy group that is more light-sensitive than compound **1**.

Finally, the electron donor was investigated. Previously, it was reported that axial ligand cleavage depended on the electron donor.[14] Thus, we used a variety of electron donors and compared the axial ligand cleavage of compounds **1**-**4** by NIR light in the presence of these donors (see Supplementary Table 1). In addition to DTT (E_{red} = −0.33 V),[15,16] we used nicotinamide adenine dinucleotide (NADH, E_{red} = −0.32 V),[17,18] cysteine (Cys, E_{red} = −0.20-−0.23 V),[16,19] glutathione (GSH, E_{red} = −0.20-−0.26 V)[16,19,20] and sodium ascorbate (NaAA, E_{red} = 0.35-0.39 V).[21,22] As a result, the efficiencies of axial ligand cleavage varied, and was independent of the redox potential and the structure of the electron donating group (see Supplementary Fig. 7). For example, although GSH and Cys have similar redox potentials and the same functional group for electron donation, axial ligands of compounds **3** and **4** were efficiently cleaved in the presence of Cys, but not GSH. Nonetheless, the efficiency of the axial ligand cleavage for each electron donor was in the order of the basicity of the axial ligand. Hence, basicity had a significant effect on light-induced axial ligand cleavage.

Discussion about development of new PIT reagents. In NIR-PIT, it is thought that

aggregation of the conjugates, which causes physical damage to the cell membrane, is induced by axial ligand cleavage of the photosensitizer. Here, we performed theoretical calculations and experiments that show the basicity of the axial ligand is involved in efficiency of the cleavage. Moreover, axial ligand cleavage of compound **2** was more light-responsive than that of compound **1**. Therefore, compound **2** having a linker for conjugation with an antibody should be a better photosensitizer than IR700. Moreover, based on the results of this study, an even better photosensitizer could be developed by modifying the axial ligand. Thus, our analysis provides useful guidelines that will assist in the development of improved photosensitizers for PIT.

Conclusions

Herein, we examined the photoinduced ligand release of IR700 derivatives with different axial ligands, such as alkoxy, siloxy, oxycarbonyl and phenoxy groups. Theoretical and experimental investigations revealed the order of basicity of the axial ligands coincided with the order of efficiency of photoinduced axial ligand cleavage. These results indicate that axial ligand cleavage is significantly influenced by protonation of the axial ligand of the anion radical. Based on the results of this study it should also be possible to design a compound whose axial ligand is cleaved with high reactivity to light.

Thus, novel PIT reagents with improved properties will be developed in the near future.

Materials and methods

Reagents and general information. General chemicals were of the best grade available, supplied by FUJIFILM Wako Pure Chemical Corporation (Osaka, Japan), Tokyo Chemical Industries Co., Ltd (Tokyo, Japan), Sigma-Aldrich Co. LLC (St. Louis, MO, USA) and KANTO CHEMICAL Co., INC. (Tokyo, Japan), and were used without further purification. NMR spectra were recorded on a JNM-ECX400P or JMN-ECS400 (JEOL Ltd., Tokyo, Japan) instrument at 400 MHz for ^{1}H NMR. δ values are given in ppm relative to tetramethylsilane or deuterated solvent signals. ESI and MALDI-TOF mass spectra (MS) were measured with a JMS-T100LP (JEOL Ltd.) and an Ultraflex II TOF/TOF (Bruker Corporation, Billerica, MA, USA), respectively. High performance liquid chromatography (HPLC) analyses and purification were performed using an HPLC system (Shimadzu Corporation, Kyoto, Japan) with reverse-phase columns, Inertsil ODS-3 (4.6 mm × 150 mm for analysis, 10 mm × 150 mm for purification) (GL Sciences Inc., Tokyo, Japan), with eluent A (0.1 M triethylammonium acetic acid (TEAA)) and eluent B (99% CH_3CN/1% H_2O).

Synthesis

Compound **1** and $SiPc(OH)_2$ were synthesized according to literature reports.[10]

Silicon Phthalocyanine Dichloride (**6**). The compound was synthesized according to a protocol described in the literature.[23] Briefly, 1,3-diiminoisoindoline **5** (176 mg, 1.2 mmol) and silicon tetrachloride (300 mg, 1.8 mmol) were dissolved in quinoline (2 mL), and the mixture was refluxed for 2 h under an Ar atmosphere. After cooling to room temperature, MeOH was added to the reaction mixture. The precipitate was collected by filtration, washed with MeOH, and dried in vacuo. The green-blue crude product was obtained and used for the next synthesis without further purification (123 mg).

Bis(4-aminobutyloxide) Silicon Phthalocyanine (**7**). Crude compound **6** (50 mg, ca. 0.082 mmol), 4-aminobutanol (73 mg, 0.82 mmol), and sodium hydride (39 mg, 1.6 mmol) were dissolved in toluene (40 mL) and the mixture was refluxed for 8 h under an Ar atmosphere. After cooling to room temperature, the reaction mixture was evaporated below 35℃. The residue was suspended with H_2O-EtOH solution (2:1), collected by filtration, washed with H_2O-EtOH solution (2:1), and dried in vacuo. A blue product was obtained (31 mg, 0.043 mmol, 52% (2 steps)). ^{1}H NMR (400 MHz, $CDCl_3$): δ −2.10 (t, J = 6.1 Hz, 4H), −1.64 (tt, J = 6.1, 7.2 Hz, 4H), −1.25 (tt, J = 7.2, 7.2 Hz, 4H), 0.94 (t, J =7.2 Hz, 4H), 8.34 (dd, J = 2.9, 5.6 Hz, 8H), 9.64 (dd, J = 2.9, 5.6 Hz, 8H). HRMS (ESI^+)

m/z: calcd for $C_{40}H_{38}N_{10}O_2Si$: 359.1470 $[M + 2H]^{2+}$; found: 359.1469.

Bis[(6-aminohexanoyl)oxide] Silicon Phthalocyanine (**8**). Crude compound **6** (300 mg, ca. 0.49 mmol), 6-aminohexanoic acid (640 mg, 4.9 mmol), and K_2CO_3 (200 mg, 1.5 mmol) were dissolved in toluene (20 mL) and the mixture was refluxed for 21 h under an Ar atmosphere. After cooling to room temperature, the reaction mixture was evaporated below 35°C. The residue was suspended in CH_2Cl_2, collected by filtration, washed with CH_2Cl_2, and dried in vacuo. A blue product was obtained (76 mg, 0.094 mmol, 14% (2 steps)). ^{1}H NMR (400 MHz, $CDCl_3$): δ −0.92-−0.89 (m, 4H), −0.79-−0.71 (m, 4H), −0.64-−0.62 (m, 4H), 0.15-0.23 (m, 4H), 1.94 (t, *J* =6.9 Hz, 4H), 8.39 (dd, *J* = 2.7, 5.7 Hz, 8H), 9.70 (dd, *J* = 2.7, 5.7 Hz, 8H). HRMS (ESI^+) m/z: calcd for $C_{44}H_{42}N_{10}O_4Si$: 401.1574 $[M + 2H]^{2+}$; found: 401.1574.

Bis(4-aminomethylphenoxide) Silicon Phthalocyanine (**9**). The compound was synthesized using the same method as described for compound **7**. 4-(Aminomethyl)phenol was used as the reagent for the axial ligand. The product was used for the next synthesis without further purification.

General procedure for alkylsulfonation. Silicon phthalocyanine with two axial ligands (30-75 mg, 0.042-0.094 mmol), 1,3-propanesultone (23-25 eq) and *N*,*N*-diisopropylethylamine (DIEA, 46-50 eq) were dissolved in MeOH (4 mL), and the

mixture was stirred at 50 ℃ for 72 h under an Ar atmosphere. The product was purified by HPLC (eluent A/eluent B = 80/20 to 50/50 in 15 min, 50/50 to 0/100 in 5 min). The product was then desalted with a Sep-Pak C18 cartridge (Waters Corp., Milford, MA, USA) and cation-exchange resin.

Bis{4-[tris(3-sulfopropyl)]ammoniobutyloxide} Silicon Phthalocyanine (**2**). The reaction yield was 20%. ^{1}H NMR (400 MHz, CD_3OD): δ −1.93 (t, J = 6.1 Hz, 4H), −1.46-−1.37 (m, 4H), −1.01-−0.91 (m, 4H), 1.32-1.50 (m, 16H), 2.53-2.64 (m, 24H), 8.53 (dd, J = 2.9, 5.7 Hz, 8H), 9.79 (dd, J = 2.9, 5.6 Hz, 8H). HRMS (ESI^-): m/z calcd for $C_{58}H_{68}N_{10}Na_3O_{20}S_6Si$:1513.2403 $[M-Na]^-$; found: 1513.2417.

Bis({6-[tris(3-sulfopropyl)]ammoniohexanoyl}oxide) Silicon Phthalocyanine (**3**). The reaction yield was 20%. ^{1}H NMR (400 MHz, CD_3OD): δ −0.69-−0.66 (m, 8H), −0.57-−0.54 (m, 4H), 0.63-0.66 (m, 4H), 1.88-1.91 (m, 12H), 2.36-2.38 (m, 4H), 2.78 (t, J = 6.3 Hz, 12H), 3.13-3.18 (m, 12H), 8.57 (dd, J = 3.0, 6.0 Hz, 8H), 9.80 (dd, J = 3.0, 6.0 Hz, 8H). HRMS (ESI^-): m/z calcd for $C_{62}H_{72}N_{10}Na_3O_{22}S_6Si$: 1597.2615 $[M-Na]^-$; found: 1597.2615.

Bis{4-[tris(3-sulfopropyl)]ammoniomethylphenoxide} Silicon Phthalocyanine (**4**). The reaction yield was 7% (3 steps). ^{1}H NMR (400 MHz, CD_3OD): δ 2.00-2.09 (m, 12H), 2.59 (d, J = 8.3 Hz, 4H), 2.70-2.81 (m, 24H), 3.71 (s, 4H), 5.84 (d, J = 8.3 Hz, 4H), 8.57

289 (dd, J = 2.8, 5.5 Hz, 8H), 9.81 (dd, J = 2.8, 5.5 Hz, 8H). HRMS (ESI^-): m/z calcd for

290 $C_{64}H_{64}N_{10}Na_3O_{20}S_6Si$: 1581.2090 $[M-Na]^-$; found: 1581.2101.

291

292 **Measurement and determination of photochemical properties.** 0.5-1.0 μM SiPc dyes

293 were dissolved in sodium phosphate buffer (pH 7.0), and the absorbance and fluorescence

294 spectra were measured using a UV spectrophotometer UV-1800 (Shimadzu Corporation)

295 and a spectrofluorometer FP-8600 (JASCO Corporation, Tokyo, Japan), respectively. The

296 relative fluorescence quantum yield (Φ_{FL}) was obtained with the following equation:

297 $$\Phi_{FL}^{sample} = \Phi_{FL}^{standard} \times \frac{F^{sample}}{F^{standard}} \times \left(\frac{n^{sample}}{n^{standard}}\right)^2 \times \frac{Abs^{standard}}{Abs^{sample}}$$

298 F denotes the area under the fluorescence band ($F = \Sigma I_{FL}(\lambda)$, where $I_{FL}(\lambda)$ is the

299 fluorescence intensity at each emission wavelength). n denotes the refractive index of the

300 solvent. Abs denotes the absorbance at the excitation wavelength. Compound **1** was used

301 as a reference (Φ_{FL} = 0.31) of the fluorescence quantum yield.

302

303 **NIR photolysis of phthalocyanine derivatives.** A solution of 5 μM phthalocyanine

304 derivatives in sodium phosphate buffer (pH 7.0) containing 1 mM DTT was prepared in

305 a vial. The solution was bubbled with Ar through the septum cap of the sealed vial before

306 being irradiated with a laser MLL-III-690 (Changchun New Industries Optoelectronics

Technology Co., Ltd, Changchun, China) (690 nm, 40 mW cm^{-2}) for 3-20 min (7.2-48 J cm^{-2}). The irradiated solution was analyzed by HPLC (eluent A/eluent B = 75/25 to 60/40 in 5 min, 60/40 to 0/100 in 10 min for compound **2**, eluent A/eluent B = 80/20 to 0/100 in 10 min for compounds **1**, **3** and **4**). The detection wavelength was 670 nm. Methylene blue (MB) was used as an internal standard. The power densities were measured with an optical power meter PM200 (Thorlabs Inc., Newton, NJ, USA). All the experiments were carried out at room temperature.

Computational details. DFT calculations were performed for the silicon phthalocyanine model compounds, **1**'-**4**', and their protonated forms using Gaussian16.[24] The LC-BLYP functional,[25] which combines the long-range corrected Becke exchange functional[26] and the Lee-Yang-Parr correlation functional[27] was employed. Spin-unrestricted Kohn-Sham self-consistent field calculations were also performed. The aug-cc-pVDZ basis set[28] was utilized for N and O atoms, while the cc-pVDZ basis set[29,30] was adopted for the other atoms. The water solvent effect was incorporated using the integral equation formalism variant of the polarizable continuum model (IEFPCM).[31] All geometries were optimized at the same level of theory and normal mode analysis was performed at the optimized structures to obtain the thermally corrected Gibbs energy at 298.15 K and 1 atm.

Data availability

The data that support the findings of this study are available from the corresponding author upon reasonable request.

Acknowledgement

This work was supported by JST-PRESTO (Grant Number: JPMJPR15P5 to M.O.), JST-CREST (Grant Number: JPMJCR1902 to M.O.) and the JSPS KAKENHI (Grant Number: JP19H03593 to M.O.), the Photo-excitonix Project in Hokkaido University, and by The Nakajima Foundation (grant to H.T.). The Institute for Chemical Reaction Design and Discovery (ICReDD) was established by the World Premier International Research Initiative (WPI), MEXT, Japan. Some calculations were performed using the computer facilities at Research Center for Computational Science, Okazaki and at Research Institute for Information Technology, Kyushu University, Japan.

Author contributions

H.T. and M.O. conceived and designed the experiments. S.M. and Y.G. performed the experiments, collected and analyzed the data. M.K., M.H. and T.T. performed

computational calculations. H.T. and M. K. wrote the paper and all authors contributed to manuscript revision and approved the final version.

Competing interests

M.O. has received research grants and consultation fees from Rakuten Medical, Inc.

Additional information

Supplementary information The online version contains supplementary material available.

Correspondence and requests for materials should be addressed to M.O.

References

1. Mitsunaga, M. et al. Cancer cell-selective in vivo near infrared photoimmunotherapy targeting specific membrane molecules. *Nat. Med.* **17**, 1685-1691 (2011).
2. Kobayashi, H. & Choyke, P. L. Near-Infrared Photoimmunotherapy of Cancer. *Acc. Chem. Res.* **52**, 2332-2339 (2019).
3. Shirasu, N., Yamada, H., Shibaguchi, H., Kuroki, M. & Kuroki, M. Potent and specific antitumor effect of CEA-targeted photoimmunotherapy. *Int. J. Cancer* **135**, 2697-2710 (2014).
4. Sato, K., Choyke, P. L. & Kobayashi, H. Photoimmunotherapy of gastric cancer peritoneal carcinomatosis in a mouse model. *PLoS One* **9**, e113276 (2014).
5. Nagaya, T. et al. Near infrared photoimmunotherapy with avelumab, an anti-programmed death-ligand 1 (PD-L1) antibody. *Oncotarget* **8**, 8807-8817 (2017).
6. Nagaya, T. et al. Near-Infrared Photoimmunotherapy Targeting Prostate Cancer with Prostate-Specific Membrane Antigen (PSMA) Antibody. *Mol. Cancer Res.* **15**, 1153-1162 (2017).
7. Nagaya, T. et al. Near Infrared Photoimmunotherapy Targeting EGFR Positive Triple Negative Breast Cancer: Optimizing the Conjugate-Light Regimen. *PLoS One* **10** (2015).

8. Takakura, H. et al. Analysis of the triplet-state kinetics of a photosensitizer for photoimmunotherapy by fluorescence correlation spectroscopy. *J. Photochem. and Photobiol. A: Chem.* **408**, 113094 (2021).
9. Kobayashi, M. et al. Theoretical and Experimental Studies on the Near-Infrared Photoreaction Mechanism of a Silicon Phthalocyanine Photoimmunotherapy Dye: Photoinduced Hydrolysis by Radical Anion Generation. *ChemPlusChem* **85**, 1959-1963 (2020).
10. Sato, K. et al. Photoinduced Ligand Release from a Silicon Phthalocyanine Dye Conjugated with Monoclonal Antibodies: A Mechanism of Cancer Cell Cytotoxicity after Near-Infrared Photoimmunotherapy. *ACS Cent. Sci.* **4**, 1559-1569 (2018).
11. Ogawa, M. et al. Immunogenic cancer cell death selectively induced by near infrared photoimmunotherapy initiates host tumor immunity. *Oncotarget* **8**, 10425-10436 (2017).
12. Nakajima, K., Takakura, H., Shimizu, Y. & Ogawa, M. Changes in plasma membrane damage inducing cell death after treatment with near-infrared photoimmunotherapy. *Cancer Sci.* **109**, 2889-2896 (2018).
13. Anderson, E. D., Sova, S., Ivanic, J., Kelly, L. & Schnermann, M. J. Defining the conditional basis of silicon phthalocyanine near-IR ligand exchange.

391 PhysChemChemPhys **20**, 19030-19036 (2018).
392 14. Anderson, E. D., Gorka, A. P. & Schnermann, M. J. Near-infrared uncaging or
393 photosensitizing dictated by oxygen tension. *Nat. Commun.* **7**, 13378 (2016).
394 15. Cleland, W. W. Dithiothreitol, a New Protective Reagent for Sh Groups. *Biochemistry*
395 **3**, 480-482 (1964).
396 16. Inaba, K. & Ito, K. Paradoxical redox properties of DsbB and DsbA in the protein
397 disulfide-introducing reaction cascade. *EMBO J.* **21**, 2646-2654 (2002).
398 17. Berg, J. M., Tymoczko, J. L. & Stryer, L. *Biochemistry* (W.H. Freeman and Co. ;
399 [Palgrave], 2002).
400 18. Zhu, X. H., Lu, M., Lee, B. Y., Ugurbil, K. & Chen, W. In vivo NAD assay reveals
401 the intracellular NAD contents and redox state in healthy human brain and their age
402 dependences. *Proc. Natl. Acad. Sci. USA* **112**, 2876-2881 (2015).
403 19. Jocelyn, P. C. The standard redox potential of cysteine-cystine from the thiol-
404 disulphide exchange reaction with glutathione and lipoic acid. *Eur. J. Biochem.* **2**,
405 327-331 (1967).
406 20. Aslund, F., Berndt, K. D. & Holmgren, A. Redox potentials of glutaredoxins and other
407 thiol-disulfide oxidoreductases of the thioredoxin superfamily determined by direct
408 protein-protein redox equilibria. *J. Biol. Chem.* **272**, 30780-30786 (1997).

21. Matsui, T., Kitagawa, Y., Okumura, M. & Shigeta, Y. Accurate standard hydrogen electrode potential and applications to the redox potentials of vitamin C and NAD/NADH. *J. Phys. Chem. A* **119** (2015).

22. Lovander, M. D. et al. Critical Review—Electrochemical Properties of 13 Vitamins: A Critical Review and Assessment. *J. Electrochem. Soc.* **165**, G18-G49 (2018).

23. Davison, J. B. & Wynne, K. J. Silicon Phthalocyanine-Siloxane Polymers: Synthesis and 1H Nuclear Magnetic Resonance Study. *Macromolecules* **11**, 186-191 (1978).

24. Gaussian 16 Rev. C.01 (Wallingford, CT, 2016).

25. Iikura, H., Tsuneda, T., Yanai, T. & Hirao, K. A long-range correction scheme for generalized-gradient-approximation exchange functionals. *J. Chem. Phys.* **115**, 3540-3544 (2001).

26. Becke, A. D. Density-functional exchange-energy approximation with correct asymptotic behavior. *Phys. Rev. A Gen. Phys.* **38**, 3098-3100 (1988).

27. Lee, C., Yang, W. & Parr, R. G. Development of the Colle-Salvetti correlation-energy formula into a functional of the electron density. *Phys. Rev. B Condens. Matter.* **37**, 785-789 (1988).

28. Kendall, R. A., Dunning, T. H. & Harrison, R. J. Electron affinities of the first-row atoms revisited. Systematic basis sets and wave functions. *J. Chem. Phys.* **96**, 6796-

6806 (1992).

29. Dunning, T. H. Gaussian basis sets for use in correlated molecular calculations. I. The atoms boron through neon and hydrogen. *J. Chem. Phys.* **90**, 1007-1023 (1989).

30. Woon, D. E. & Dunning, T. H. Gaussian basis sets for use in correlated molecular calculations. III. The atoms aluminum through argon. *J. Chem. Phys.* **98**, 1358-1371 (1993).

31. Mennucci, B., Cancès, E. & Tomasi, J. Evaluation of Solvent Effects in Isotropic and Anisotropic Dielectrics and in Ionic Solutions with a Unified Integral Equation Method: Theoretical Bases, Computational Implementation, and Numerical Applications. *J. Phys. Chem. B* **101**, 10506-10517 (1997).

Figures

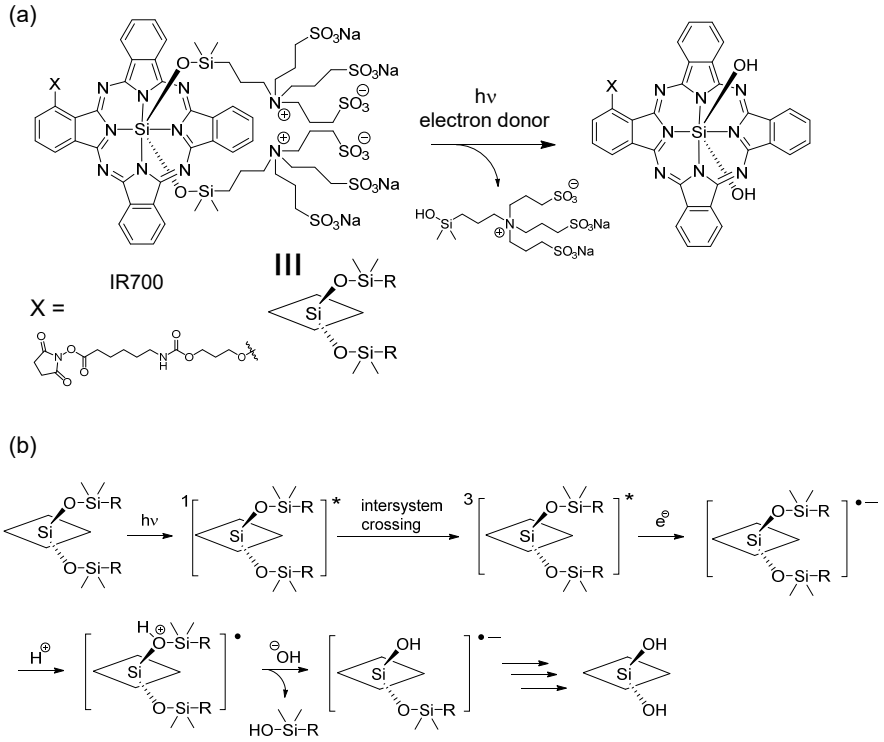

Fig. 1 Photochemical reaction in photoimmunotherapy (a) Axial ligand cleavage of IRDye700DX (IR700), a photosensitizer for photoimmunotherapy. Cleavage is induced by NIR light in the presence of an electron donor, and the hydrophobic compound is generated by loss of the hydrophilic axial ligands. (b) Plausible mechanism of axial ligand cleavage of IR700. Upon absorbance of excitation light, IR700 is excited to the singlet state. Some of the singlet state are transferred to the triplet state, resulting in generation of an anion radical by electron transfer from an electron donor. Next, stepwise reaction of the axial ligand involving water, such as protonation and ligand exchange, occur spontaneously. Finally, IR700 derivatives with the axial ligand cleaved are generated.

(a)

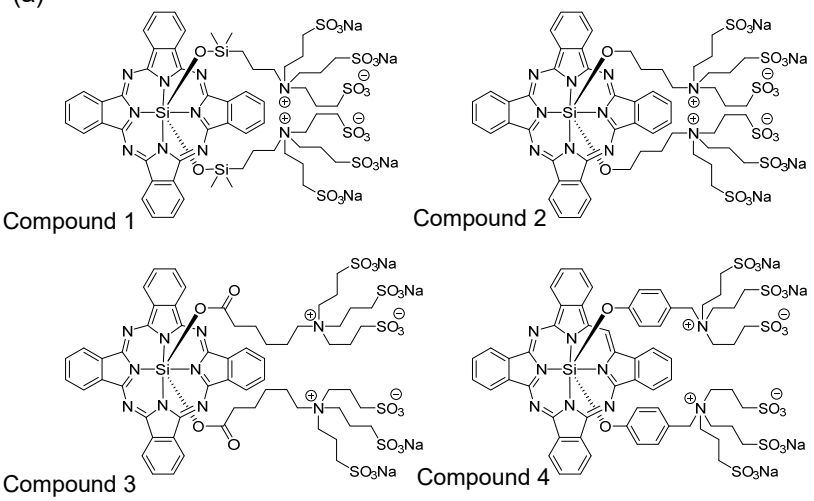

(b)

$$[SiPcY_2]^{\bullet-} + H_3O^+ \xrightarrow{\Delta G} [SiPc(YH)Y]^{\bullet} + H_2O$$

Compound	1’	2’	3’	4’
Y=	$OSiMe_3$	OEt	OCOEt	OPh
ΔG (kJ/mol)	–143.0	–147.6	–103.5	–106.8

Fig. 2 Computational calculation of silicon phthalocyanines with different axial ligands (a) Structures of compounds **1-4**. (b) Calculated *ΔG* (at 298.15 K, 1 atm) of protonation to the oxygen atom on the Si-O bond (ULC-BLYP/cc-pVDZ, diffuse functions were augmented to N and O atoms, in water solvent).

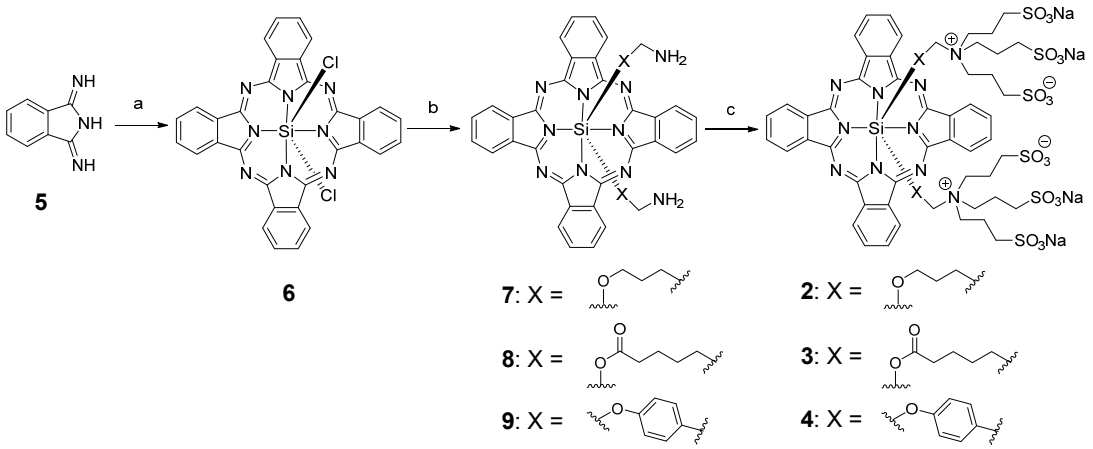

Fig. 3 Synthetic scheme for compounds 2-4. (a) $SiCl_4$, quinoline, (b) appropriate amines, NaH or K_2CO_3, toluene, (c) sultone, *i*Pr_2EtN, MeOH.

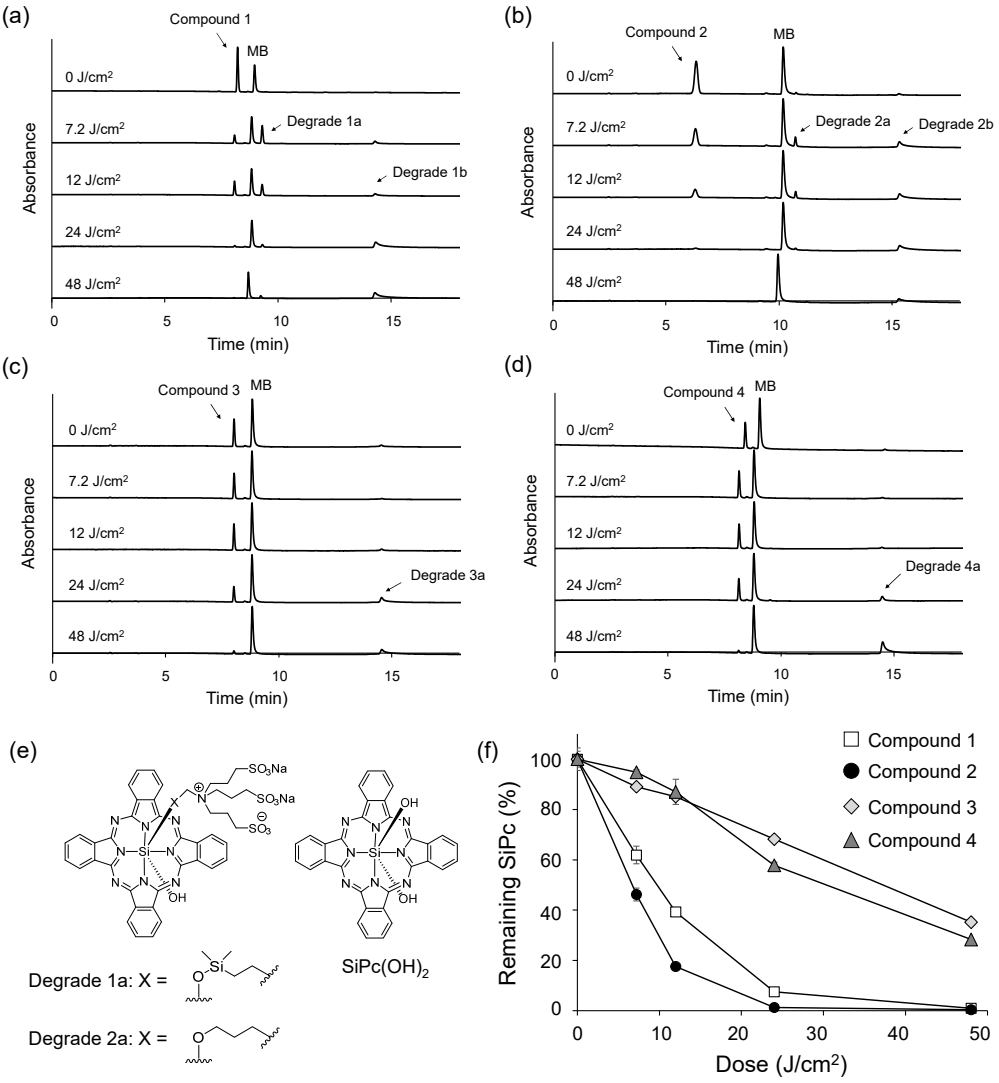

Fig. 4. HPLC analysis of photolysis by NIR light. Compounds **1**-**4** in the deoxygenated solution with 1 mM DTT were irradiated by NIR light (690 nm) for the indicated times and the solution was analyzed by HPLC with methylene blue (MB) as an internal standard. (a) compound **1**, (b) compound **2**, (c) compound **3** and (d) compound **4**. (e) Chemical structures of the degradation products after photolysis. (f) The ratio of absorbance peak area compared to the sample before irradiation. Data represents the mean ±SEM (n = 3).

Table 1. Absorbance/emission wavelengths ($\lambda_{abs}/\lambda_{em}$), molar extinction coefficient (ε) and fluorescence quantum yields (Φ_{FL}) of compounds 1-4.

Compound	λ_{abs} /nm[a]	λ_{em} /nm[a]	$\varepsilon \times 10^5$/L mol^{-1} cm^{-1}		Φ_{FL}
			H_2O	DMSO	
1	677	684	1.9	2.4	0.31[b]
2	684	690	1.7	2.0	0.30
3	691	699	1.9	2.5	0.27
4	689	695	1.7	2.0	0.29

[a] Absorption/emission wavelengths were obtained from Fig. S2. [b] Ref 8.

Supplementary Files

This is a list of supplementary files associated with this preprint. Click to download.

- SupportingInformationNIRCommunChem.pdf